

Reactivity of Chilean Reservoir Rocks and the Use of Geochemical Tools for Reservoir Characterization

Fabian Nitschke¹, Sebastian Held¹, Niklas Mundhenk¹, Ignacio Villalon², Thomas Kohl¹, Thomas Neumann¹

¹Karlsruhe Institute of Technology (KIT) - Institute of Applied Geosciences (AGW), Germany

²Andean Geothermal Center of Excellence (CEGA), Santiago, Chile

1. Introduction

Chile has a huge potential for the utilization of geothermal energy that is associated with active volcanism. This resource has remained largely untapped so far but efforts on geothermal exploration have been increased recently and are also part of this study.

The study area is located in the vicinity of the Mt. Villarrica in Southern Chile, which is one of the most active volcanoes of Chile (ORTIZ 2003). Numerous hot springs can be found in the surrounding area that indicate a large geothermal system (Fig. 1). As part of the South Volcanic Zone Mt. Villarrica belongs to a NW-SE striking chain of three major stratovolcanoes (Villarrica-Quetrupillan-Lanín). This chain and a related parallel fault zone crosscut and offset the major N-S striking Liquiñe-Ofqui fault zone (LOFZ) (CEMBRANO et al. 1996) by a few kilometers at the surface (ROSENAU et al. 2006). In the Villarrica area, a large number of natural hot springs distributes over an area of 2000 km². Temperatures of thermal waters at the outlets do not exceed 80 °C and reservoir temperatures determined using $\delta^{18}\text{O}$ isotopes of SO₄ and H₂O to be about 130-140°C (HELD et al. 2015).

The tectonic situation, including the over >1000 km N-S extending LOFZ, may be responsible for the presence of a high number of geothermal springs. Furthermore a change in basement geology is observed. South of the volcanic chain granitoid basement rocks are present, including the tonalite used in this study (part of the North Patagonian Batholith). North of the volcanic chain those granitoid basement rocks are continuously replaced by a volcano-sedimentary unit called Cura-Mallín formation that contains the porphyric andesite used.

The purpose of the ongoing KIT-CEGA collaborative research project MultiGeoEx is to establish diverse geochemical (source-rock deduction,

geothermometry) and geophysical exploration methods (e.g. magnetotellurics) to assess the impact of the volcano and cross-cutting major fault zones on subsurface fluid migration.

Within a broader context of geothermal exploration the aim of this work is to study the geochemical characteristics of natural fluids, which have been in contact to reservoir rocks, in order to derive information about the subsurface conditions (temperature, fluid migration paths, mineralogy of the reservoir). Because it is expected that the natural geothermal fluids carry distinct chemical signatures, fluid-rock-experiments have been performed in the laboratory. The results can assist to better understand the reactivity of these rocks and enable to test the application of geochemical tools, such as source-rock deduction and geothermometry. Preliminary results from the experimental campaign are presented and tested in this particular geological setting.

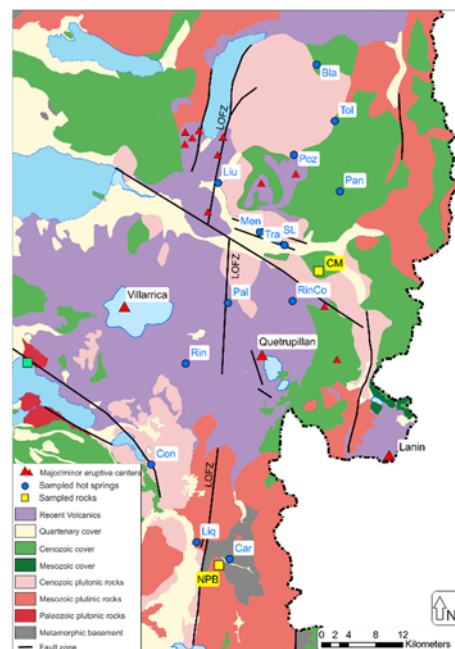


Fig. 1 Geological map of the area (the rock sampling locations are indicated in yellow; CM: andesite, NPB: tonalite)

2. Material, Methods & Experimental design

Batch-type experiments were performed with two different rock samples that are, due to their stratigraphic location and their relatively high permeability, presumed to be the reservoir rocks for the discharging fluids: (1) a Mesozoic tonalite and (2) a Cenozoic porphyric andesite, the first being more siliceous and less aluminous than the latter. The bulk rock composition (X-ray fluorescence) and mineralogy (thin-section microscopy and X-ray diffraction) are given in Tab. 1.

Before the experiments the rock samples were ground with an agate disc mill and sieved to get the $<63\text{ }\mu\text{m}$ grain size fraction. BET measurements revealed SSA of 2.1 (tonalite) and 3.6 m^2/g (andesite), respectively. 40 g of rock powder was transferred to a stainless-steel reactor which was completely filled up with pure H_2O , creating far-from-equilibrium conditions with respect to the minerals present. The experiments are designed to achieve an equilibrium conditions between the rock and the fluid. The rock/water ratio (by wt.%) was approx. 0.3. In accordance with results from oxygen isotopic geothermometry on spring discharges in the Villarrica region (HELD et al. 2015), the reaction temperature was chosen to be 140 °C. In order to keep track of the reaction progress, the fluid was sampled and analyzed after 1, 2, 4, 6, 10, 20, 30, 45, 60, 90, 120, and 180 days. Each time step is represented by an autonomous experiment.

Table 1 Compositions of the rock samples determined by XRF and XRD.

	Tonalite	Andesite
Composition		
SiO ₂	67.8	54.6
[mass-%]		
K ₂ O	2.3	1.5
CaO	2.6	8.1
Fe ₂ O ₃	5.0	7.8
Mineralogy		
Quartz	48	-
Chalcedony	-	5
Plagioclase	28	40
Pyroxene	-	30
[vol.-%]		
Serizite	12	-
Muscovite	2	-
Chlorite	< 5	5
Biotite	8	-
Clays	-	10
Magnetite	-	10

Fluid composition was measured by inductively coupled plasma mass spectrometry (ICP-MS) for the cations and by ion chromatography (IC) for the anions. Silicon concentration was determined by spectrophotometry.

3. Results and Discussion

The experimental results obtained show that a considerable net mass transfer into the fluid occurs right from the beginning of the experiments. Total dissolved solids (TDS) of the withdrawn fluids approach 1000 ppm. As can be seen in the Durov diagram, the experiments produce different fluids in terms of composition, pH, and TDS (Fig. 2), mostly associated with a significant SO_4^{2-} release. Interestingly, the release over time differs significantly for the two rock types. The tonalite powder starts with a very high TDS in the early phase of the experiment before dropping to lower values. Afterwards an increase towards higher TDS values can be discerned again. The andesite experiments show an opposing trend with a relatively steady increase in the early phase of the experiment and a slight drop after 100 days.

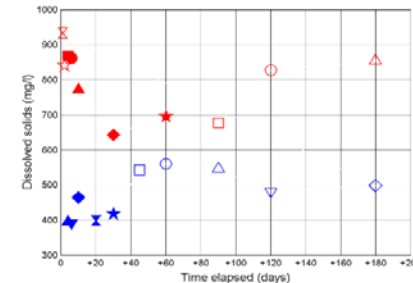
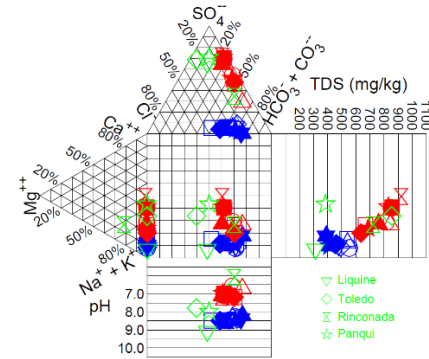


Fig. 2 (top) Durov diagram for the experimentally produced fluids and natural geothermal fluids; (bottom) TDS vs. time (red: tonalite; blue: andesite, green: geothermal springs).

The difference in bulk reactivity gives rise to the assumption that different mechanisms are involved. The high initial release for the tonalite powder might be associated with the rapid dissolution of μm sized particles and other highly reactive sites on the mineral surfaces as well as desorption. These processes are often observed in mineral dissolution studies (Bertrand et al. 1994). However, given the "identical" sample preparation, this cannot explain the lower release in comparison with the andesite powder. Also this contradicts the differences in the BET values, which is higher for the andesite powder.

The release of the major cations and silica, as well as the pH is depicted in Fig. 3. The concentration of Na increases steadily to several mmol/l. Silica reaches quartz and chalcedony saturation, respectively. The other solutes do not significantly exceed 2 mmol/l, except for Ca in an early stage of the experiment.

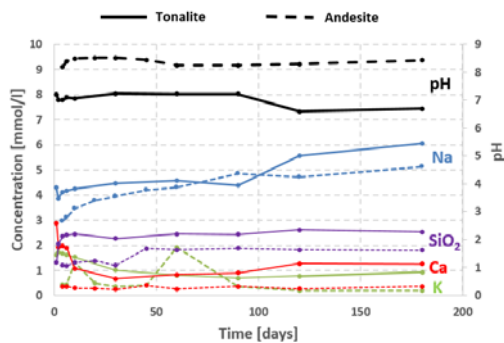


Fig. 3 Concentrations of the major cations, silica, and pH over the course of the experiments.

Solution compositions were plotted on activity-activity diagrams to illustrate the reaction path followed by the solution and to obtain information about secondary phases that may (or may not) form during the course of the experiments. It is evident from the activity-activity plot in Fig. 4 that the two experimental series produce two separate point clouds that are distinct by different pH values and silica concentrations.

The clustering indicates that we are not necessarily looking on actual reaction progress, but rather on some final state of reaction. Further SEM/EDX investigation will reveal whether the indicated phases do occur as secondary phases.

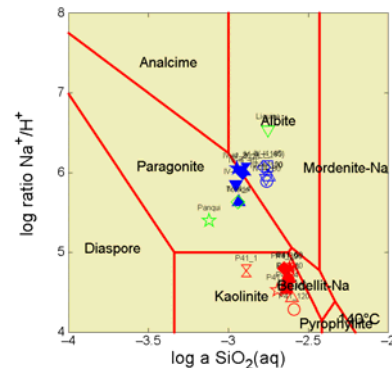


Fig. 4 Plot of $\log (a_{\text{Na}^+}/a_{\text{H}^+})$ vs. $\log a \text{SiO}_2(\text{aq})$ for the two experimental series (red: tonalite; blue: andesite) and natural geothermal fluids (green).

3.1 Source rock deduction

One aim of this work is to test whether fluids from natural springs can be unambiguously attributed to a distinct source rock. A system consisting of a fluid and a rock being in contact over a sufficiently long period of time is expected to reach a chemical equilibrium state for a given temperature. Hence, chemical compositions from discharged natural fluids should reflect the mineral assemblage of the reservoir rock.

Evaluation of experimental data show that fluids resulting from alteration of both presumed reservoir rocks can be distinguished due to their different composition. The Durov plot (Fig. 2) as well as the Na-phase stability plot (Fig. 4) show a considerable clustering. An assignment of the natural fluids to one of both groups however is at the current stage of investigations more difficult. Several aspects, which has not taken into account, affecting the natural fluids like the contribution of meteoric water (initial conditions), mixture of different geothermal fluids, precipitation and dissolution processes during the upstream from reservoir or the possible volcanic impact. Therefore more research has to be done.

3.2 Geothermometry

Geothermometry is a powerful tool in order to estimate the reservoir temperature at which the fluid was equilibrated. Many geothermometer for various settings and temperature environments exist (GIGGENBACH 1988, ARNORSSON et al. 1983, FOUILLAG & MICHARD 1981, FOURNIER 1977,)

among which the silica, the K/Mg, and the Na/K geothermometer have been tested in this study. Since the temperature of the experiments is fixed, it can be verified, whether certain geochemical geothermometer yield reliable temperature estimates or not.

The dissolution of silica from the tonalite occurs rapidly and concentrations of around 2.5 mmol/l are reached after approximate 100 days (Fig. 5). The andesite releases silica much slower and concentrations remain below 1.8 mmol/l. The achieved concentration levels coincide with the calculated solubilities of quartz and chalcedony at this temperature (horizontal lines). Presumably, their precipitation limits the concentration in the fluid. Surprisingly, the granite with primary quartz reaches chalcedony solubility, while the tuff with primary chalcedony only reaches quartz saturation.

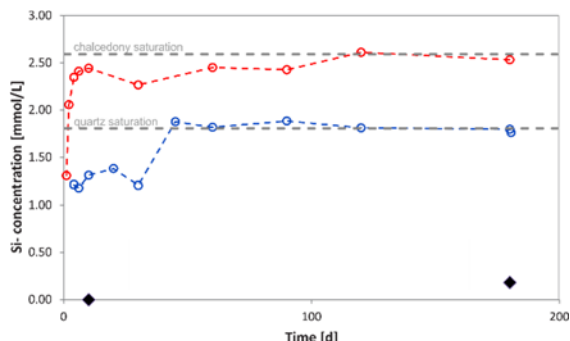


Fig. 5 Silica concentration vs. time for the two experimental series; the horizontal lines represent the calculated quartz (lower line) and chalcedony (upper line) saturations for 140 °C (blue: andesite, red: tonalite).

The K/Mg geothermometer belongs to the family of cation geothermometers and relies on the equilibration of Mg containing phyllosilicates such as chlorites and biotite and K-feldspars (Giggenbach, 1988). In this study it has been tested for the two experimental series. Fig. 6 shows the concentrations (in mg/l) of K and Mg (multiplied by ten) over the course of the experiment and the calculated temperature according to the given equation. The black horizontal line marks the temperature at which the experiment has been performed.

$$\text{K/Mg - Geothermometer: } T[\text{°C}] = \frac{4410}{14.0 - \log \frac{C(K^2)}{C(Mg)}} - 273.15 \quad \text{GIGGENBACH 1988}$$

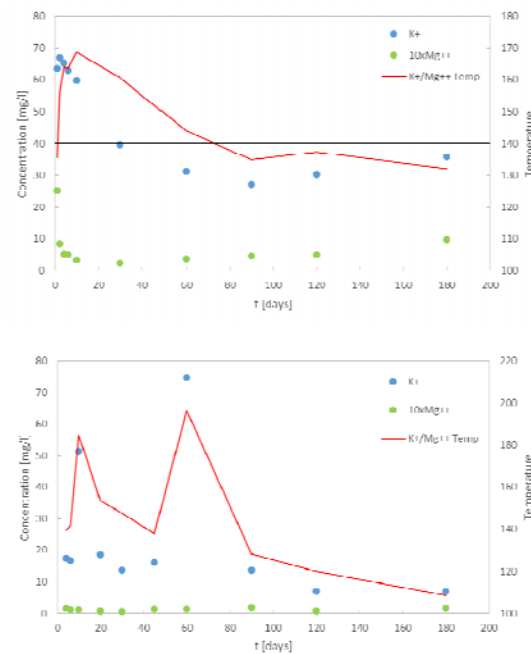


Fig. 6 Concentrations of K and Mg (multiplied by ten) over the course of the experiment; the red lines mark the calculated temperature according to the given equation; the horizontal black line marks the temperature of the experiment.

For the tonalite experiments we observed a very good agreement of the calculated geothermometer temperature and the experimental temperature of 140°C. For the andesite, however, the agreement between the two temperatures is poor. The actual temperature is significantly underestimated by approx. 30°C. The K and Mg values are relatively stable (except for two outliers in the K concentration for the andesite experimental series). To really test the applicability for the rock types more experiments at different temperatures have to be done and will be performed soon.

Acknowledgements

The study is part of a collaborative research project between the Karlsruhe Institute of Technology (KIT) and the Andean Geothermal Center of Excellence (CEGA). The study is supported by the CONICYT-BMBF International Scientific Collaborative Research Program project PCCI130025/FKZ 01DN14033.

References

ARNORSSON S., GUNNL AUGSSON E. and SVAVARSSON H. (1983): The chemistry of geothermal waters in Iceland. III. Chemical geothermometry in geothermal investigations. *Geochim. Cosmochim. Ac.* 47: 567-577.

BERTRAND C., FRITZ B. and SUREAU J.F. (1994): Hydrothermal experiments and thermos-kinetic modelling of water-sandstone interactions. *Chem. Geol.* 116:189-202.

CEMBRANO J., HERVÉ F. and LAVENU A. (1995): The Liquine Ofqui fault zone: a long-lived intra-arc fault system in southern Chile. *Tectonophysics* 259: 55-66.

FOUILLAC R. and MICHARD S. (1981): Sodium/Lithium ratio in water applied to geothermometry of geothermal reservoirs. *Geothermics* 10: 55-70.

FOURNIER R.O. (1977): Chemical Geothermometers and Mixing Models for Geothermal Systems. *Geothermics* 5: 41-50.

GIGGENBACH W. F. (1988): Geothermal solute equilibria. Derivation of Na-K-Mg-Ca geoindicators. *Geochim. Cosmochim. Ac.* 52: 2749-2765.

HELD B., SCHILL E., SANCHEZ P., NEUMANN T., EMMERICH K., MORATA D. and KOHL T. (2015): Geological and Tectonic Settings Preventing High-Temperature Geothermal Reservoir Development at Mt. Villarrica (Southern Volcanic Zone): Clay Mineralogy and Sulfate-Isotope Geothermometry. *Proceedings World Geothermal Congress 2015*, Melbourne, Australia, 19-25 April 2015.

ORTIZ R., MORENO H., GARCIA A., FUENTEALBA G., ASTIZ M., PENA P., SANCHEZ N and TARRAG M. (2003): Villarrica volcano (Chile): characteristics of the volcanic tremor and forecasting of small explosions by means of a material failure method. *J. Volcanol. Geotherm. Res.* 128: 247-259.

ROSENAU M., MELNICK D. and ECHTLER H. (2006): Kinematic constraints on intra-arc shear and strain partitioning in the southern Andes between 38_S and 42_S latitude. *Tectonics* 25: 4013.